Blucher Mechanical Engineering Proceedings
May 2014, vol. 1 , num. 1
www.proceedings.blucher.com.br/evento/10wccm

A NOVEL FINITE ELEMENT FORMULATION FOR LARGE DEFORMATION ANALYSIS BASED ON INCREMENTAL EQUILIBRIUM EQUATION IN CONJUNCTION WITH REZONING TECHNIQUE

Y. Onishi[1], K. Amaya[1]

[1] Department of Mechanical and Environmental Informatics, Tokyo Institute of Technology (yonishi@a.mei.titech.ac.jp)

Abstract. *A novel finite element formulation based on the incremental equilibrium equation (IEE) in conjunction with the rezoning technique is proposed. The IEE used in this study can be derived from the virtual work equation in rate form. Due to the IEE, the equilibrium between the nodal internal force and the nodal external force after a rezoning is automatically satisfied; thus, it is not necessary to solve the equilibrium again before starting the next time increment. Through some examples of large deformation analysis with the rezoning method, it is confirmed that the proposed method is enough accurate and stable.*

Keywords: *Finite element method, Incremental equilibrium equation, Large deformation, Rezoning, Static-implicit analysis*

1. INTRODUCTION

In the field of computational solid mechanics, the finite element method (FEM) is the de-facto standard approach used for extensive analysis. Although the finite element method is widely used in large deformation analysis, it is known that severe mesh distortion in large strain cases leads to reduction of accuracy and convergence failure. Improvement of finite element (FE) formulation to solve severely large strain problems, such as metal forming simulations, stably and accurately is still an issue to be resolved [1, 2].

Currently, it seems that the mesh-to-mesh solution mapping method [3] (also known as the rezoning method [4]) is the only approved conventional approach to severely large strain problems. This method, however, frequently brings convergence failure because of the temporal discontinuity of the nodal internal force between the old mesh and the new mesh in a static-implicit analysis. The conventional FE codes [3, 4] deal with this discontinuity in a manner to dissolve it by little and little over some time increments; thus, they cannot avoid error accumulation nor frequent convergence failure. It seems difficult to completely resolve this discontinuity issue as long as the standard FE formulation is adopted.

Meanwhile, we recently proposed a new Galerkin meshfree formulation based on the incremental equilibrium equation (IEE) [5]. The IEE was developed for Galerkin meshfree methods with the updated Lagrangean procedure to resolve the temporal discontinuity of the nodal internal force between the old and the new moving least square (MLS) supports, and it brought out high performances in stability and accuracy in large deformation analysis for elastic and elastoplastic bodies. It would appear that this discontinuity issue is essentially identical to that in the FE rezoning method mentioned above. However, the IEE is still a semi-empirical equation without any mathematical derivation [5] and verified only in the meshfree formulation. To derive the IEE mathematically and to apply it for the FE rezoning method should be important.

In this paper, we firstly present a mathematical derivation of the IEE, which has not been presented so far, in Section 2. Secondly, a novel FE formulation for large deformation analysis based on the IEE with rezoning technique is described in Section 3. Thirdly, some examples of analysis with the proposed FE formulation with the rezoning method in comparison to the standard FE formulation without rezoning are shown in Section 4. Finally, we conclude that the proposed FE formulation with the rezoning method has enough accuracy as much as the standard FE formulation and has the potential to completely overcome the discontinuity issue in the conventional rezoning method.

2. DERIVATION OF INCREMENTAL EQUILIBRIUM EQUATION

One form of the virtual work equation for solid mechanics [6] is written as

$$\int_{\Omega(t)} \dot{\mathbf{\Pi}}_t^T(t) : \delta \boldsymbol{F}_t(t)\, \mathrm{d}\Omega = \int_{\Gamma(t)} \dot{\underline{\boldsymbol{t}}}_t(t) \cdot \delta \boldsymbol{u}\, \mathrm{d}\Gamma + \int_{\Omega(t)} \rho \dot{\boldsymbol{g}} \cdot \delta \boldsymbol{u}\, \mathrm{d}\Omega, \tag{1}$$

where $\dot{\square}$ denotes the material time derivatives, $\Omega(t)$ is the current domain, $\Gamma(t)$ is the current boundary, $\mathbf{\Pi}_t(t)$ is the first Piola–Kirchhoff stress tensor in the current configuration, $\delta \boldsymbol{F}_t(t)$ is the variation of the deformation gradient tensor in the current configuration, $\underline{\boldsymbol{t}}_t(t)$ is the surface traction vector in the current configuration, $\delta \boldsymbol{u}$ is the variation of the displacement vector, ρ is the density, and $\boldsymbol{g}$ is the body force vector.

The material time derivatives in Eq. (1) can be approximated as

$$\dot{\mathbf{\Pi}}_t^T(t) \simeq \Delta \mathbf{\Pi}_t^T / \Delta t, \quad \dot{\underline{\boldsymbol{t}}}_t(t) \simeq \Delta \underline{\boldsymbol{t}}_t / \Delta t, \quad \dot{\boldsymbol{g}} \simeq \Delta \boldsymbol{g} / \Delta t, \tag{2}$$

by applying temporal linearization during a time increment, Δt. At the same time, the variations in Eq. (1) can be approximated by applying the Galerkin method with finite elements as

$$\delta \boldsymbol{F}_t(t) \simeq \mathcal{F}_{9\times1}^{3\times3}\big([B_{\mathrm{N}}]\{\delta u\}\big), \quad \delta \boldsymbol{u} \simeq [N]\{\delta u\}, \tag{3}$$

where $\{\delta u\}$ is the variation of the nodal displacements in the column vector form, $[N]$ is the shape function in the matrix form given by

$$[N] = \begin{bmatrix} N_1 & 0 & 0 & \cdots & N_j & 0 & 0 & \cdots \\ 0 & N_1 & 0 & \cdots & 0 & N_j & 0 & \cdots \\ 0 & 0 & N_1 & \cdots & 0 & 0 & N_j & \cdots \end{bmatrix}, \tag{4}$$

$[B_{\mathrm{N}}]$ is the matrix given by

$$[B_{\mathrm{N}}] = \begin{bmatrix} \frac{\partial N_1}{\partial x} & 0 & 0 & \cdots & \frac{\partial N_j}{\partial x} & 0 & 0 & \cdots \\ 0 & \frac{\partial N_1}{\partial y} & 0 & \cdots & 0 & \frac{\partial N_j}{\partial y} & 0 & \cdots \\ 0 & 0 & \frac{\partial N_1}{\partial z} & \cdots & 0 & 0 & \frac{\partial N_j}{\partial z} & \cdots \\ \frac{\partial N_1}{\partial y} & 0 & 0 & \cdots & \frac{\partial N_j}{\partial y} & 0 & 0 & \cdots \\ \frac{\partial N_1}{\partial z} & 0 & 0 & \cdots & \frac{\partial N_j}{\partial z} & 0 & 0 & \cdots \\ 0 & \frac{\partial N_1}{\partial x} & 0 & \cdots & 0 & \frac{\partial N_j}{\partial x} & 0 & \cdots \\ 0 & \frac{\partial N_1}{\partial z} & 0 & \cdots & 0 & \frac{\partial N_j}{\partial z} & 0 & \cdots \\ 0 & 0 & \frac{\partial N_1}{\partial x} & \cdots & 0 & 0 & \frac{\partial N_j}{\partial x} & \cdots \\ 0 & 0 & \frac{\partial N_1}{\partial y} & \cdots & 0 & 0 & \frac{\partial N_j}{\partial y} & \cdots \end{bmatrix}, \tag{5}$$

and $\mathcal{F}_{9\times1}^{3\times3}$ is the function to convert a 9-component column vector to a 3×3 matrix.

By substituting Eq. (2) and (3) into Eq. (1) and by erasing Δt and $\{\delta u\}$, the following discretized equilibrium equation for the fully implicit time advancing in the incremental form is obtained.

$$\{\Delta f^{\mathrm{ext}}\} - \{\Delta f^{\mathrm{int}}\} = \{0\}, \tag{6}$$

where $\{\Delta f^{\mathrm{ext}}\}$ and $\{\Delta f^{\mathrm{int}}\}$ are the nodal external force vector increment and the nodal internal force vector increment, respectively, defined as follows.

$$\{\Delta f^{\mathrm{ext}}\} = \sum_{s\in\mathbb{S}} \int_{\Gamma_s^+} [N^+]^T \{\Delta \underline{t}_t\} \,\mathrm{d}\Gamma + \sum_{e\in\mathbb{E}} \int_{\Omega_e^+} \rho^+ [N^+]^T \{\Delta g\} \,\mathrm{d}\Omega, \tag{7}$$

$$\{\Delta f^{\mathrm{int}}\} = \sum_{e\in\mathbb{E}} \int_{\Omega_e^+} [B_{\mathrm{N}}^+]^T \{\Delta \Pi_t^T\} \,\mathrm{d}\Omega, \tag{8}$$

where $\square^+$ denotes the state after the time increment, $\mathbb{S}$ is the set of elemental faces shaping the domain boundary, $\mathbb{E}$ is the set of elements in the domain, Γ_s is the domain boundary shaped by an elemental face s, and Ω_e is the domain of an element e. In addition, $\{\Delta \underline{t}_t\}$, $\{\Delta g\}$, and $\{\Delta \Pi_t^T\}$ are the column vector representations of $\Delta \underline{\boldsymbol{t}}_{\boldsymbol{t}}$, $\Delta \boldsymbol{g}$, and $\Delta \boldsymbol{\Pi}_t^T$, respectively. In order to avoid the error accumulation in the practical implementation, the equation to solve is arranged as

$$(\{f^{\mathrm{ext}}\} + \{\Delta f^{\mathrm{ext}}\}) - (\{f^{\mathrm{int}}\} + \{\Delta f^{\mathrm{int}}\}) = \{0\}. \tag{9}$$

Hereafter, Eq. (9) is called as the incremental equilibrium equation (IEE) in this paper. Since the IEE is derived from one of the common virtual work equations, the IEE is mathematically identical to the standard equilibrium equation, $\{f^{\mathrm{ext}}\} - \{f^{\mathrm{int}}\} = \{0\}$.

3. FE FORMULATION BASED ON IEE WITH REZONING

3.1. Advantage of the proposed FE formulation

As described in Section 1, the conventional rezoning method based on the standard equilibrium equation frequently brings convergence failure because of the temporal discontinuity of $\{f^{\mathrm{int}}\}$ between the old mesh and the new mesh in a static-implicit analysis. Namely, even if $\{f^{\text{ext}}\} - \{f^{\text{int}}\} = \{0\}$ is well satisfied after a time increment, once the rezoning is carried out, $\{f^{\text{ext}}\} - \{f^{\text{int}}\} = \{0\}$ is no longer satisfied. This unbalanced force is generally not so small to be ignored in comparison to the tolerance; thus, convergence failure sometimes occurs no matter how small Δt is chosen for the next time increment.

In contrast, the original form of the IEE shown in Eq. (6) can be evaluated separately for each individual time increment; thus, the temporal discontinuity does not exist in principle. By adjusting $\{f^{\text{ext}}\}$ and $\{f^{\text{int}}\}$ so that $\{f^{\text{ext}}\} - \{f^{\text{int}}\} = \{0\}$ is satisfied at the end of the rezoning procedure, the IEE shown in Eq. (9) can be used without regard to the temporal discontinuity. Hence, the advantage of the proposed FE formulation to be described below is to stabilize the FE rezoning with minimum error accumulation in the static-implicit analysis.

3.2. Constitutive equations

In the following discussion, for simplicity, we focus on the Hencky's elastic body [7–9] described with the following constitutive equations:

$$\overset{\circ}{\boldsymbol{T}} = \boldsymbol{C}_{\text{L}} : \boldsymbol{D} \quad \Big(\text{i.e., } \boldsymbol{T} = \boldsymbol{C}_{\text{L}} : \boldsymbol{E}\Big), \tag{10}$$

where $\overset{\circ}{\boldsymbol{T}}$ is the Jaumann rate of the Cauchy stress, $\boldsymbol{D}$ is the stretching tensor, $\boldsymbol{T}$ is the Cauchy stress tensor, $\boldsymbol{E}$ is the Hencky strain tensor, and $\boldsymbol{C}_{\text{L}}$ is the 4th order elasticity tensor described as

$$C_{ijkl} = \lambda\delta_{ij}\delta_{kl} + 2\mu\delta_{ik}\delta_{jl}, \tag{11}$$

where λ and μ are the Lame's parameters.

3.3. Flowchart of the formulation

The flowchart of the proposed FE formulation is shown in Fig. 1. The flow is basically the same as that of the standard FE formulation except the calculation parts of $\{\Delta f^{\text{ext}}\}$, $\{\Delta f^{\text{int}}\}$, the equation to solve, and the rezoning part.

3.4. Calculation of $\{\Delta f^{\text{int}}\}$

At the beginning of the Newton–Raphson loop, all the velocity-related variables of the integration points such as $\overline{\boldsymbol{L}}$, $\overline{\boldsymbol{D}}$, and $\overline{\boldsymbol{W}}$ are calculated in the same fashion as the standard FEM [10]:

$$\{\overline{L}\}\Delta t \simeq [\overline{B_{\text{N}}}]\{\Delta u\}, \quad \{\overline{D}\}\Delta t \simeq [\overline{B_{\text{L}}}]\{\Delta u\}, \quad \overline{\boldsymbol{W}} = \overline{\boldsymbol{L}} - \overline{\boldsymbol{D}}, \tag{12}$$

where $\overline{\square}$ denotes the average value in the time increment, $\boldsymbol{L}$ is the velocity gradient tensor, $\boldsymbol{W}$ is the spin tensor, and $[B_{\text{L}}]$ is the matrix given by

$$[B_{\text{L}}] = \begin{bmatrix} \frac{\partial N_1}{\partial x} & 0 & 0 & \cdots & \frac{\partial N_j}{\partial x} & 0 & 0 & \cdots \\ 0 & \frac{\partial N_1}{\partial y} & 0 & \cdots & 0 & \frac{\partial N_j}{\partial y} & 0 & \cdots \\ 0 & 0 & \frac{\partial N_1}{\partial z} & \cdots & 0 & 0 & \frac{\partial N_j}{\partial z} & \cdots \\ \frac{\partial N_1}{\partial y} & \frac{\partial N_1}{\partial x} & 0 & \cdots & \frac{\partial N_j}{\partial y} & \frac{\partial N_j}{\partial x} & 0 & \cdots \\ 0 & \frac{\partial N_1}{\partial z} & \frac{\partial N_1}{\partial y} & \cdots & 0 & \frac{\partial N_j}{\partial z} & \frac{\partial N_j}{\partial y} & \cdots \\ \frac{\partial N_1}{\partial z} & 0 & \frac{\partial N_1}{\partial x} & \cdots & \frac{\partial N_j}{\partial z} & 0 & \frac{\partial N_j}{\partial x} & \cdots \end{bmatrix}. \tag{13}$$

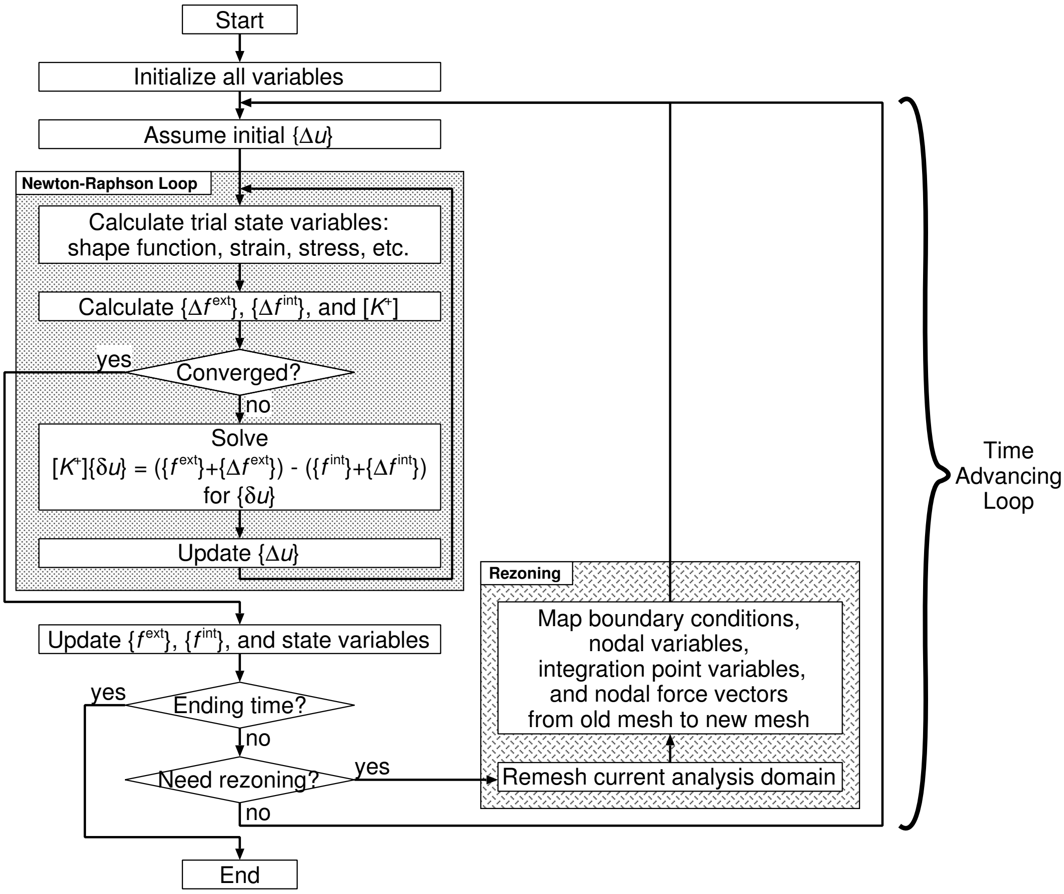

Figure 1. Flowchart of static-implicit finite element formulation based on incremental equilibrium equation (IEE) in conjunction with rezoning technique.

With regard to the definition of the Jaumann rate [6]

$$\overset{\circ}{\boldsymbol{T}} \equiv \dot{\boldsymbol{T}} - (\boldsymbol{W} \cdot \boldsymbol{T} - \boldsymbol{T} \cdot \boldsymbol{W}), \tag{14}$$

the Cauchy stress tensor after the time increment $\boldsymbol{T}^{+}$ can be approximately calculated as

$$\boldsymbol{T}^{+} \simeq \boldsymbol{T} + \boldsymbol{C}_{\mathrm{L}} : \overline{\boldsymbol{D}}\Delta t + (\overline{\boldsymbol{W}} \cdot \widetilde{\boldsymbol{T}} - \widetilde{\boldsymbol{T}} \cdot \overline{\boldsymbol{W}})\Delta t, \tag{15}$$

where $\widetilde{\boldsymbol{T}}$ is the approximated average Cauchy stress tensor in the time increment calculated as

$$\widetilde{\boldsymbol{T}} = \boldsymbol{T} + \frac{1}{2}\boldsymbol{C}_{\mathrm{L}} : \overline{\boldsymbol{D}}\Delta t + \frac{1}{2}(\overline{\boldsymbol{W}} \cdot \boldsymbol{T} - \boldsymbol{T} \cdot \overline{\boldsymbol{W}})\Delta t. \tag{16}$$

Hence, the Cauchy stress tensor increment is obtained as $\Delta\boldsymbol{T} = \boldsymbol{T}^{+} - \boldsymbol{T}$.

Meanwhile with regard to $\boldsymbol{T}^{T} = \boldsymbol{T}$ and the following relational expression [6]

$$\dot{\boldsymbol{\Pi}}_{t} \equiv \dot{\boldsymbol{T}} + \mathrm{tr}(\boldsymbol{L})\boldsymbol{T} - \boldsymbol{L} \cdot \boldsymbol{T}, \tag{17}$$

$\Delta\boldsymbol{\Pi}_{t}^{T}$ can be approximately represented with $\Delta\boldsymbol{T}$ as

$$\Delta\boldsymbol{\Pi}_{t}^{T} \simeq \Delta\boldsymbol{T} + \mathrm{tr}(\overline{\boldsymbol{L}})\boldsymbol{T}\Delta t - \boldsymbol{T} \cdot \overline{\boldsymbol{L}}^{T}\Delta t. \tag{18}$$

Consequently, $\{\Delta f^{\mathrm{int}}\}$ can be calculated by substituting Eq. (18) into Eq. (8).

3.5. Calculation of $[K^{+}]$

By substituting $\dot{\boldsymbol{T}}$ of Eq. (14) into that of Eq. (17) and by transposing the both sides, we obtain the following equation:

$$\dot{\boldsymbol{\Pi}}_t^T = \boldsymbol{C}_{\mathrm{L}} : \boldsymbol{D} + (\boldsymbol{W} \cdot \boldsymbol{T} - \boldsymbol{T} \cdot \boldsymbol{W}) + \mathrm{tr}(\boldsymbol{L})\boldsymbol{T} - \boldsymbol{T} \cdot \boldsymbol{L}^T. \tag{19}$$

By simplifying the 2nd and later terms of the right-hand side of Eq. (19) with $\boldsymbol{L}$ and forming it into the column vector form, we obtain

$$\{\dot{\Pi}_t^T\} = \mathcal{F}_{6\times1}^{9\times1}\big([C_{\mathrm{L}}]\{D\}\big) + [C_{\mathrm{N}}]\{L\}, \tag{20}$$

where $[C_{\mathrm{N}}]$ is the matrix given by

$$[C_{\mathrm{N}}] = \begin{bmatrix} 0 & T_{xx} & T_{xx} & 0 & 0 & -T_{xy} & 0 & -T_{zx} & 0 \\ T_{yy} & 0 & T_{yy} & -T_{xy} & 0 & 0 & 0 & 0 & -T_{yz} \\ T_{zz} & T_{zz} & 0 & 0 & -T_{zx} & 0 & -T_{yz} & 0 & 0 \\ T_{xy} & 0 & T_{xy} & \frac{T_{yy}-T_{xx}}{2} & \frac{T_{yz}}{2} & \frac{-T_{yy}-T_{xx}}{2} & \frac{-T_{zx}}{2} & \frac{-T_{yz}}{2} & \frac{-T_{zx}}{2} \\ T_{zx} & T_{zx} & 0 & \frac{T_{yz}}{2} & \frac{T_{zz}-T_{xx}}{2} & \frac{-T_{yz}}{2} & \frac{-T_{xy}}{2} & \frac{-T_{zz}-T_{xx}}{2} & \frac{-T_{xy}}{2} \\ 0 & T_{xy} & T_{xy} & \frac{-T_{yy}-T_{xx}}{2} & \frac{-T_{yz}}{2} & \frac{-T_{yy}+T_{xx}}{2} & \frac{T_{zx}}{2} & \frac{-T_{yz}}{2} & \frac{-T_{zx}}{2} \\ T_{yz} & T_{yz} & 0 & \frac{-T_{zx}}{2} & \frac{-T_{xy}}{2} & \frac{T_{zx}}{2} & \frac{T_{zz}-T_{yy}}{2} & \frac{-T_{xy}}{2} & \frac{-T_{zz}-T_{yy}}{2} \\ 0 & T_{zx} & T_{zx} & \frac{-T_{yz}}{2} & \frac{-T_{zz}-T_{xx}}{2} & \frac{-T_{yz}}{2} & \frac{-T_{xy}}{2} & \frac{-T_{zz}+T_{xx}}{2} & \frac{T_{xy}}{2} \\ T_{yz} & 0 & T_{yz} & \frac{-T_{zx}}{2} & \frac{-T_{xy}}{2} & \frac{-T_{zx}}{2} & \frac{-T_{zz}-T_{yy}}{2} & \frac{T_{xy}}{2} & \frac{-T_{zz}+T_{yy}}{2} \end{bmatrix} \tag{21}$$

and $\mathcal{F}_{6\times1}^{9\times1}$ is the function to convert a 6-component column vector of a symmetric stress to a 9-component column vector of an asymmetric stress. Thus, $\{\Delta\Pi_t^T\}$ can be represented as

$$\{\Delta\Pi_t^T\} = \mathcal{F}_{6\times1}^{9\times1}\big([C_{\mathrm{L}}]\{\overline{D}\}\Delta t\big) + [C_{\mathrm{N}}]\{\overline{L}\}\Delta t. \tag{22}$$

By substituting Eq. (22) into Eq. (8) with regard to Eq. (12) and by differentiating it with $\{\Delta u\}$, we obtain the approximate stiffness matrix $[K^{+}]$ $\big(= \frac{\partial\{\Delta f^{\mathrm{int}}\}}{\partial\{\Delta u\}}\big)$:

$$[K^{+}] = \sum_{e\in\mathbb{E}} \int_{\Omega_e^{+}} [B_{\mathrm{L}}^{+}]^T[C_{\mathrm{L}}][\overline{B_{\mathrm{L}}}] + [B_{\mathrm{N}}^{+}]^T[C_{\mathrm{N}}][\overline{B_{\mathrm{N}}}]\,\mathrm{d}\Omega. \tag{23}$$

The approximate stiffness matrix $[K^{+}]$ given by Eq. (23) is an asymmetric matrix. If the computer memory consumption must be saved, a symmetrized matrix $[\underset{\sim}{K^{+}}]$ $\big(= \frac{[K^{+}]+[K^{+}]^T}{2}\big)$ can be utilized.

3.6. Rezoning procedure

The rezoning procedure consists of the remeshing part and the mapping part. In case there are multiple closed domains as the analysis domain, the rezoning procedure should be performed for each closed domain individually.

3.6.1 Remeshing

The remeshing procedure is as same as that of the standard FE formulation. We employed a commercial software, GAMBIT [11], for the mesh generation. The coarseness and fineness of the new mesh is controlled by the size functions [11].

3.6.2 Mapping

The mapping procedure is almost the same as that of the standard FE formulation except the mapping of the nodal force vectors to be described.

a) Mapping of boundary conditions The boundary conditions given on the boundaries of the old mesh (old boundaries) are mapped to the boundaries of the new mesh (new boundaries).

b) Mapping of nodal states The nodal states such as the initial position vector, the displacement vector, etc. stored at the nodes of the old mesh (old nodes) are mapped to the nodes of the new mesh (new nodes) through the following steps. The first step is to find the old element that includes each new node; the second step is to interpolate the nodal states using the shape function of the found element. Note that the mapping of the nodal force vectors is an exception to this rule, as described later.

c) Mapping of integration point states The integration point states such as the stress tensors, the strain tensors, etc. stored at the integration points of the old mesh (old integration points) are mapped to the integration points of the new mesh (new integration points) through the following steps. The first step is to interpolate or extrapolate the old integration point states to the old nodes; the second step is to find the old element that includes each new integration point; the third step is to interpolate the integration point states using the shape function of the found element.

d) Mapping of nodal force vectors Unlike the other nodal states, the nodal force vectors of the old nodes are mapped to the new nodes through the following special way. Firstly, the nodal force vectors at all the new inner nodes are set to zero vectors; thus, the values to be determined are the nodal force vectors at all the new boundary nodes, $\{f^{\#\Gamma}\}$. Secondly, the nodal force vectors at the new nodes that have some kind of loading boundary conditions assigned are set to the assigned values. The rest of the undetermined values in $\{f^{\#\Gamma}\}$ are determined so that the following cost function is minimized.

$$\sum_{s \in \mathbb{S}^{\#}} \left\| \boldsymbol{t}_s^{\#}(\{f^{\#\Gamma}\}) - \boldsymbol{t}_s \right\|^2 \longrightarrow \min, \tag{24}$$

where $\Box^{\#}$ denotes the variable of the new mesh, $\boldsymbol{t}_s$ is the surface traction vector at the center position of the new elemental face s. Finally, $\{f^{\#\mathrm{ext}}\}$ is constructed of the nodal force vectors at all the new nodes and let $\{f^{\#\mathrm{int}}\} \longleftarrow \{f^{\#\mathrm{ext}}\}$ so that Eq. (9) is automatically satisfied at the beginning of the next time increment. This elimination of the residual of the IEE, which induces little error accumulation, is done only at the end of each rezoning.

4. EXAMPLES OF ANALYSIS

For the stability and accuracy verification of the proposed method, a few examples of analysis under the plane strain condition are shown in this section.

4.1. Uniaxial tension analysis

Figure 2 shows the outline of the uniaxial tension analysis under the two-dimensional plane strain condition. The material of the domain is the Neo-Hookean hyperelastic material [3] of $C_{10} = 0.17240$ GPa and $D_1 = 0.60006$ GPa^{-1}. The left side is horizontally constrained, the lower side is vertically constrained, and the upper side is horizontally constrained and vertically displaced 1 m in the upward direction statically. The analysis span is treated as a 100 s timespan for convenience, and the timespan is discretized into 100 equal time steps.

The elements used in this analysis are all 1st-order triangular elements. The number of nodes and elements are 527 and 972, respectively. The solutions of this problem using the proposed formulation with the rezoning method and the standard formulation without rezoning are provided for comparison. The rezoning is carried out every 10 s, i.e., every 10th step.

Figure 3 shows the deformed shapes and Mises stress distributions at 0.0 and 1.0 m enforced displacement states. Although the standard formulation succeeds in getting the converged result, accuracy of the result cannot be high because of the severe element distortion. In contrast, the proposed formulation succeeds in getting the converged result through 9 rezonings without any severe element distortion.

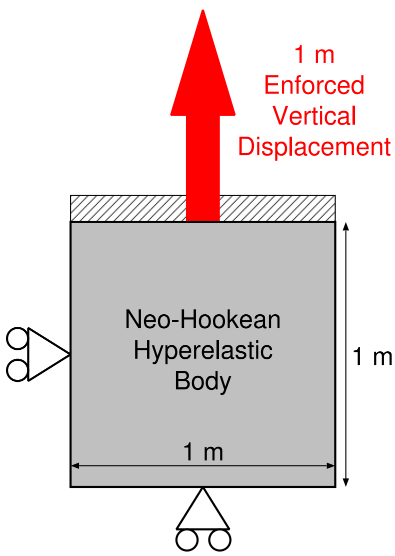

Figure 2. Outline of the uniaxial tension analysis.

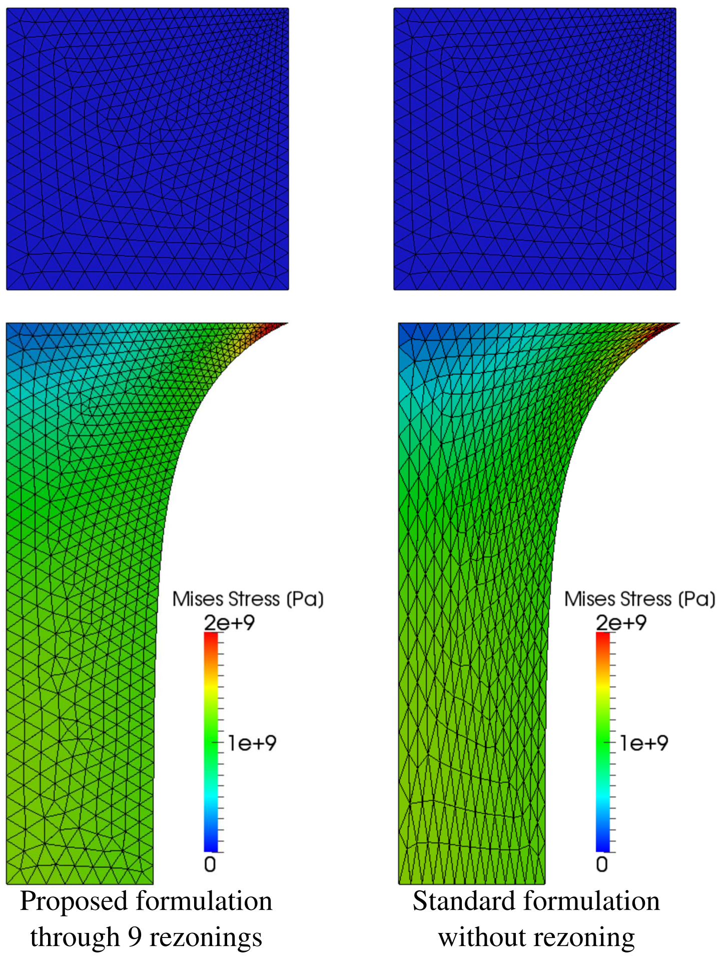

Figure 3. Deformation and Mises stress distribution of the uniaxial tension analysis at 0.0 and 1.0 m enforced displacement states.

4.2. Shearing analysis

Figure 4 shows the outline of the shearing analysis under the two-dimensional plane strain condition. The material of the domain is the Hencky's elastic material of 1 GPa Young's modulus and 0.3 Poisson's ratio, i.e., $\lambda = 0.576923$ GPa and $\mu = 0.384615$ GPa. The lower side up to 2 m from the left is perfectly constrained, and the upper side up to 2 m from the right is horizontally constrained and displaced 5 m in the vertical downward direction statically. The analysis span is treated as a 500 s timespan for convenience, and the timespan is discretized into 923 unequal time steps with automatic time step control.

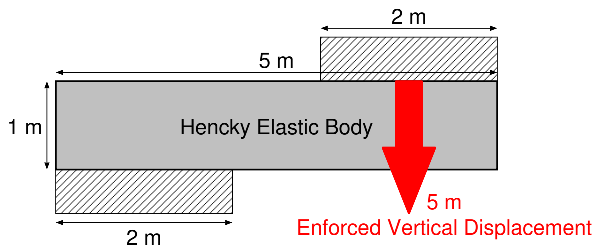

Figure 4. Outline of the uniaxial tension analysis.

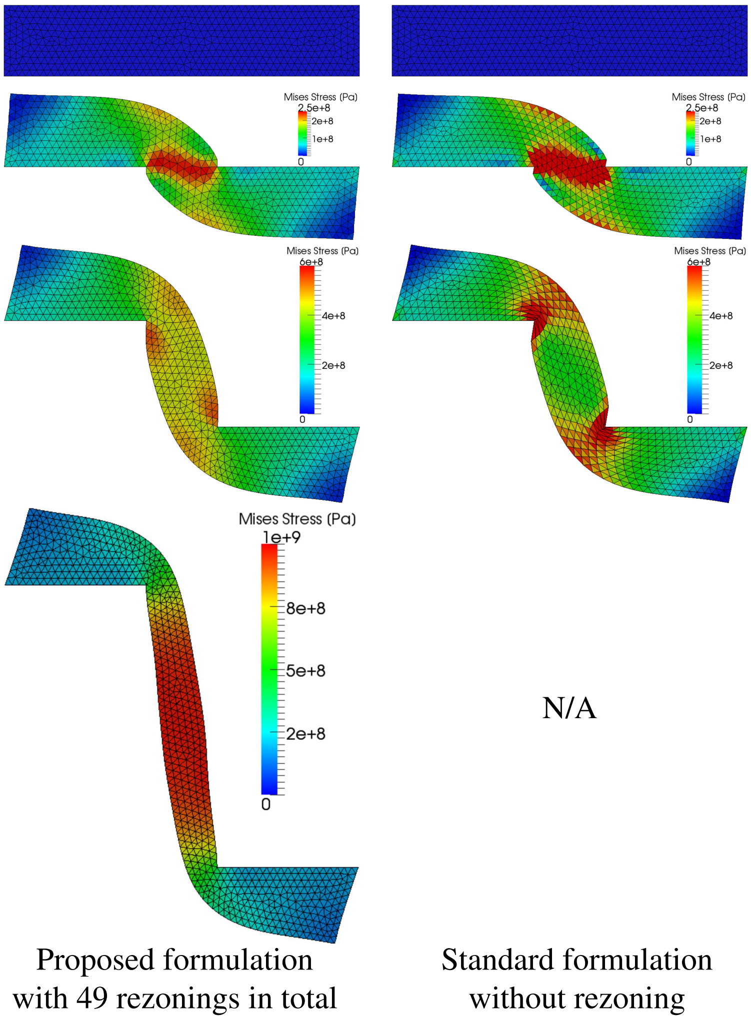

Figure 5. Deformation and Mises stress distribution of the shearing analysis at 0.0, 1.0, 2.5, and 5.0 m enforced displacement states.

The elements used in this analysis are all 1st-order triangular elements. The number of nodes and elements are 622 and 1,122, respectively. The solutions of this problem using the proposed formulation with the rezoning method and the standard formulation without rezoning are provided for comparison. The rezoning is carried out every 10 s.

Figure 5 shows the deformed shapes and Mises stress distributions at 0.0, 1.0, 2.5, and 5.0 m enforced displacement states. The analysis of the standard formulation without rezoning brings convergence failure right after 2.5 m enforced displacement because of the severe element distortion. In contrast, the analysis of the proposed formulation succeeds in getting the converged result through 49 rezonings, and the deformed shape and the Mises stress distribution seem appropriate.

5. CONCLUSION

A novel finite element formulation based on the incremental equilibrium equation (IEE) in conjunction with the rezoning technique was proposed. A mathematical derivation of the IEE from the virtual work equation in rate form was presented. The proposed FE formulation with the rezoning method was precisely described and its advantage over the conventional FE rezoning formulation was clarified. A few examples of the large deformation analysis were presented to show the accuracy and stability of the proposed method. Further improvements would make the proposed method an efficient method for the practical metal forming simulations with severely large deformations.

6. REFERENCES

[1] Zienkiewicz O. C., Huang G. C., and Liu Y. C., "Adaptive fem computation of forming processes – application to porous and non-porous materials,". *International Journal for Numerical Methods in Engineering*, 30, 1527–1553, 1990.

[2] Cheng J. H. and Kikuchi N., "A mesh re-zoning technique for finite element simulations of metal forming processes,". *International Journal for Numerical Methods in Engineering*, 23, 219–228, 1986.

[3] SIMULIA Inc. , *ABAQUS 6.8 Documentation*. SIMULIA Inc., 2008.

[4] MSC.Software Corp. , *MARC 2010 Theory and User Information*. MSC.Software Corp., 2010.

[5] Onishi Y. and Amaya K., "Floating stress-point integration meshfree method for large deformation analysis of elastic and elastoplastic materials,". *International Journal for Numerical Methods in Engineering*, 2012 (In Press).

[6] Hisada T. and Noguchi H., *Basis and Application of Non-linear Finite Element Method (in Japanese)*. Maruzen, 1995.

[7] Gurtin M. E. and Spear K., "On the relationship between the logarithmic strain rate and the stretching tensor,". *International Journal of Solids and Structures*, 19(5), 437–444, 1983.

[8] Hoger A., "The material time derivative of logarithmic strain,". *International Journal of Solids and Structures*, 22(9), 1019–1032, 1986.

[9] Anand L., "A rate constitutive equation for moderate strain isotropic elasticity,". *Mechanics Research Communications*, 11(5), 345–352, 1984.

[10] Zienkiewicz O. C., *The Finite Element Method for Solid and Structural Mechanics 6th Ed.* Elsevier, 2005.

[11] ANSYS Inc. , *GAMBIT 2.4 Documentation*. ANSYS Inc., 2007.